

Frascati Physics Series Vol. XLVI (2007), pp. 000-000  
 HADRON07: XII INT. CONF. ON HADRON SPECTROSCOPY – Frascati, October 8-13, 2007  
 Parallel Session

**Studies of Exclusive  $e^+e^- \rightarrow \text{hadrons}$  Reactions with Baryons and Strange Particles Using Initial State Radiation at Babar**

S.I.Serednyakov, for Babar Collaboration  
*Budker Institute of Nuclear Physics,*  
*Novosibirsk State University,*  
*630090, Novosibirsk, Russia*

**Abstract**

New *BABAR* results on exclusive  $e^+e^- \rightarrow \text{hadrons}$  reactions at low c.m. energy with a baryon-antibaryon or  $K\bar{K}$  pair in the final state are presented. Cross sections are measured using the initial state radiation technique from the threshold up to 4–5 GeV. From the measured  $e^+e^- \rightarrow p\bar{p}, \Lambda\bar{\Lambda}, \Sigma^0\bar{\Sigma}^0, \Lambda\bar{\Sigma}^0(\Sigma^0\bar{\Lambda})$  cross sections we derive effective baryon form factors and compare them with predictions. We measure the  $K\bar{K}\pi(\eta), K^+K^-\pi\pi, K^+K^-3\pi, K^+K^-4\pi, K^+K^-K^+K^-$  final states and also study their internal structure. A new  $Y(2175)$  state is observed in  $e^+e^- \rightarrow K^+K^-f_0(980)$ , with  $f_0 \rightarrow \pi\pi$ . The total measured  $e^+e^-$  annihilation cross section into final states including strange baryons or strange mesons is estimated to be 10% of the full hadronic cross section.

**Introduction.** The  $e^+e^- \rightarrow \text{hadrons}$  reactions with a pair of baryons or strange mesons in the final state are the subject of the experimental study for many years for several reasons. First, they give considerable contribution

into the total  $e^+e^-$  hadronic cross section. Second, from the two body cross section one can derive electromagnetic timelike form factors. And last but not least, new states can reveal themselves in the study of these reactions.

In this work a sample of *BABAR* <sup>1)</sup> data corresponding to  $230 fb^{-1}$  is analyzed. We search for initial state radiation (ISR) processes  $e^+e^- \rightarrow f + \gamma$ , where  $\gamma$  is a high energy photon with  $E_\gamma > 3 GeV$  and  $f$  is a hadronic system with the mass  $m$ . (A description of ISR approach is given in <sup>2)</sup>). Through ISR the wide mass range (from  $2m_\pi$  to  $\sim 10 GeV/c^2$ ) is studied in a single experiment with full efficiency and full angular acceptance beginning from the very threshold. For example, in the reaction  $e^+e^- \rightarrow p\bar{p}\gamma$ , the protons produced at the threshold already have the laboratory momenta  $\geq 1 GeV/c$ .

The ISR approach, applied to B-factories data, is quite competitive with direct  $e^+e^-$  experiments, because the effective ISR luminosity is comparable with already stored  $e^+e^-$  luminosity. The following final states are studied in this work:  $p\bar{p}$ ,  $\Lambda\bar{\Lambda}$ ,  $\Sigma^0\bar{\Sigma}^0$ ,  $\Lambda\bar{\Sigma}^0(\Sigma^0\bar{\Lambda})$  with baryons and  $K\bar{K}\pi(\eta)$ ,  $K^+K^-\pi\pi$ ,  $K^+K^-3\pi$ ,  $K^+K^-4\pi$ ,  $K^+K^-K^+K^-$  and other with kaons. Other ISR results are covered in the talk <sup>3)</sup>.

**Baryon pair production results.** The cross section for the  $e^+e^- \rightarrow B\bar{B}$  process, where  $B$  is a spin-1/2 baryon has the form:

$$\sigma_{B\bar{B}}(m) = \frac{4\pi\alpha^2\beta}{3m^2} \left[ |G_M(m)|^2 + \frac{1}{2\tau}|G_E(m)|^2 \right], \quad (1)$$

where  $\beta = \sqrt{1 - 4m_B^2/m^2}$ ,  $\tau = m^2/4m_B^2$ ,  $G_E$  and  $G_M$  are the electric and magnetic form factors. From the total cross section (1) the values of the  $G_E$  and  $G_M$  can not be extracted separately. Therefore, the effective form factor  $|F(m)|$  is introduced as  $|F(m)|^2 = (2\tau|G_M(m)|^2 + |G_E(m)|^2)/(2\tau + 1)$ . The modulus  $|G_E/G_M|$  is determined from the  $\cos\theta_B$  distribution, where  $\theta_B$  is the polar angle of the baryon with respect to the  $e^-$  beam in the  $e^+e^-$  c.m. frame. The  $\sin^2\theta_B$  term in this distribution is proportional to  $|G_E|^2$  and the  $1 + \cos^2\theta_B$  term - to  $|G_M|^2$ . Fitting of the  $\cos\theta_B$  distribution then gives the  $|G_E/G_M|$  ratio.

The  $e^+e^- \rightarrow p\bar{p}$  results <sup>2)</sup> are shown in Figs.1,2,3. The measured cross section (Fig.1) is flat at the threshold while the form factor sharply rises in this region (Fig.2). It has two step-like structures: at 2.15 and 2.9 GeV. The ratio  $|G_E/G_M|$  (Fig.3) is found to be  $\geq 1$  in contradiction with previous works.

The measured  $e^+e^- \rightarrow \Lambda\bar{\Lambda}$  cross section (Fig.6) <sup>5)</sup> agrees with the only

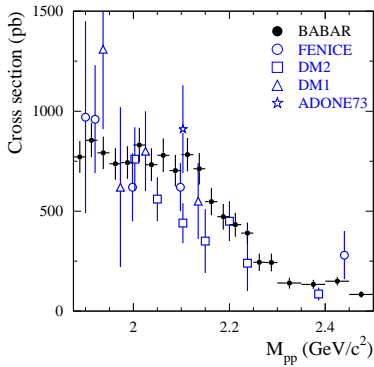


Figure 1: The  $e^+e^- \rightarrow p\bar{p}$  cross section near threshold.

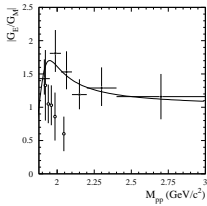


Figure 3: The  $G_E/G_M$  ratio for proton.

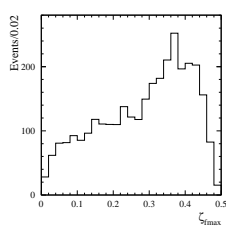


Figure 4: The simulated  $\Lambda$  polarization.

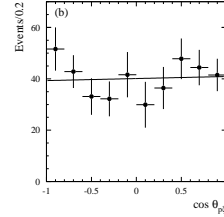


Figure 5: The measured  $\cos\theta_{pC}$  distribution.

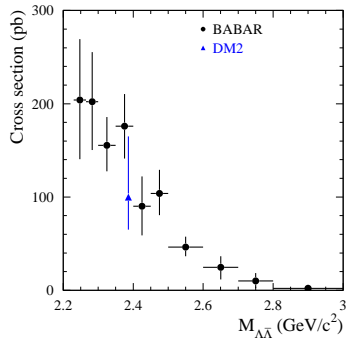


Figure 6: The  $e^+e^- \rightarrow \Lambda\bar{\Lambda}$  cross section.

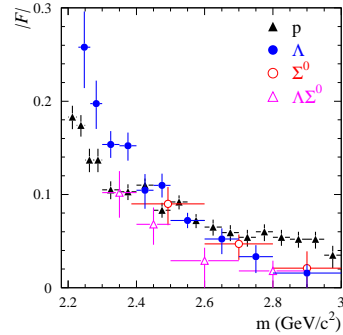


Figure 7: The measured proton,  $\Lambda$ ,  $\Sigma^0$  and  $\Lambda\Sigma^0$  form factors.

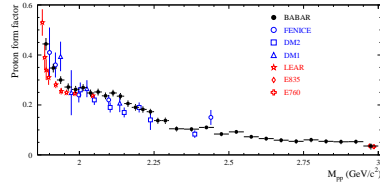


Figure 2: The proton timelike form factor data.

previous measurement <sup>4)</sup>. 200 found  $\Lambda\bar{\Lambda}$  events are selected by using  $\Lambda \rightarrow p\pi$  decay. The measured  $\Lambda$  effective form factor is shown in Fig.7. The ratio  $G_E/G_M$  for the  $\Lambda$  baryon is consistent with unity. Use of the  $\Lambda \rightarrow p\pi$  decay allows to measure the relative phase  $\phi$  between the complex  $G_E$  and  $G_M$  form factors. The transverse polarization  $\zeta$  of outgoing baryons is proportional to  $\sin\phi$ . The measurement of  $\zeta$  is done from the angular spectrum of protons in the  $\Lambda \rightarrow p\pi$  decay. The simulated distribution over  $\zeta_{max}$  is shown in Fig.4. The measured  $\cos\theta$  distribution, where  $\theta$  is the angle between the  $\Lambda$  polarization and the proton momentum from the  $\Lambda \rightarrow p\pi$  decay in the  $\Lambda$  rest frame, is shown in Fig.5. No  $\cos\theta$  asymmetry is seen. The following limits on the  $\Lambda$  polarization  $-0.22 < \zeta < 0.28$  and the phase  $-0.76 < \sin\phi < 0.98$  are obtained. The limit on  $\sin\phi$  is too weak to make any certain conclusion on the phase  $\phi$  between the  $G_E$  and  $G_M$  for the  $\Lambda$  hyperon.

In a similar way the  $e^+e^- \rightarrow \Sigma^0\bar{\Sigma}^0$  and  $e^+e^- \rightarrow \Sigma^0\bar{\Lambda}(\Lambda\bar{\Sigma}^0)$  cross sections are measured. For detection of  $\Sigma^0$ , the decay chain  $\Sigma^0 \rightarrow \Lambda\gamma \rightarrow p\pi\gamma$  is used. About 20 candidate events are selected for each reaction. The effective  $\Sigma^0$  and  $\Sigma^0\Lambda$  form factors are shown in Fig.7. It is seen that  $\Lambda$ ,  $\Sigma^0$  and  $\Sigma^0\Lambda$  form factors are of the same order.

**SU(3) and QCD tests for baryon form factors.** New *BABAR* data on baryon form factors give a possibility to compare them with the predictions from the known form factors models. A fit with the asymptotic QCD fitting function <sup>6)</sup>

$$F \sim \alpha_S^2(m^2)/m^4 \sim C/m^4 \ln^2(m^2/\Lambda^2), \quad (2)$$

applied to the proton form factor data, is shown in Fig.8. Here  $\Lambda = 0.3 \text{ GeV}$ , and  $C$  is a free parameter. If we neglect the steps at 2.15 and 2.9 GeV, the fit (2) in Fig.8 describes the data fairly well, indicating the asymptotic behaviour already at  $2 \div 3 \text{ GeV}$ .

The same fit (2) for the  $\Lambda$  form factor is not so good (see the curve labeled  $n = 4$  in the Fig.9). The fit improves if we take power  $m^8$  in the denominator of Eq.2 instead of  $m^4$  (Fig.9, curve  $n = 8$ ). The same results hold in the fitting of the  $\Sigma^0$  and  $\Sigma^0\Lambda$  formfactors. We conclude that  $\Lambda$ ,  $\Sigma^0$  and  $\Sigma^0\Lambda$  form factors are considerably steeper than the proton form factor.

In SU(3) symmetry model the octet baryon form factors are related to each other. The asymptotic predictions <sup>7)</sup> are:  $F_n = 1.94F_\Lambda$ ,  $F_p = 2.13F_n$ ,  $F_{\Sigma^0} = -1.18F_\Lambda$ ,  $F_p = 4.1F_\Lambda$ . A test of these predictions in Fig.10

for the doubled *BABAR*  $\Lambda$  <sup>5)</sup> and Fenice neutron <sup>8)</sup> form factors at 2.4 GeV shows good agreement with prediction  $F_n = 1.94F_\Lambda$ . This result is important for the planned neutron form factor measurement <sup>9)</sup>. The comparison of the proton and  $\Lambda$  form factors in Fig.11, shows that the data at  $E < 3$  GeV are far from the asymptotic QCD prediction  $F_p = 4F_\Lambda$ . But the course of both form factors with energy indicates that above 4 GeV the agreement with the QCD predictions is expected.

**Final states including kaon pairs.** The ISR approach is also applied to study  $e^+e^-$  annihilation cross sections with a pair of kaons in the final state. Figure 12 shows the  $e^+e^- \rightarrow K_S K^\pm \pi^\mp$  cross section <sup>10)</sup> with a peak at  $\sim 1.7$  GeV mainly from the  $\phi'(1680)$  state. The Dalitz plot in Fig.13 shows that  $KK^*(892)$  and  $KK_2^*(1430)$  intermediate states dominate in the  $K\bar{K}\pi$  final state. The fitting of the  $e^+e^- \rightarrow K\bar{K}\pi$  cross sections with the sum of the expected contributions from the  $\phi, \phi', \phi'', \rho^0, \rho', \rho''$  state is done. The parameters of the  $\phi'$  and other excited vector meson states, obtained from the fit, are compatible with their PDG values.

In the cross section of the  $e^+e^- \rightarrow \phi\eta, \eta \rightarrow \gamma\gamma$  process (Fig.14) the peak from the  $\phi'(1680)$  is seen. Another small peak is observed with  $M = 2139 \pm 35$  MeV,  $\Gamma = 76 \pm 62$  MeV and  $2\sigma$  significance. In general the  $e^+e^- \rightarrow \phi\eta$  channel is very suitable for a search of  $\phi'$ 's states, because it is entirely isoscalar and a contribution of  $\omega$ 's states is OZI suppressed. Another channel  $e^+e^- \rightarrow \phi\pi^0$  is potentially suitable for a search of exotic states, because the ordinary vector mesons decays into  $\phi\pi^0$  are strongly OZI suppressed. The  $e^+e^- \rightarrow \phi\pi^0$  cross section is measured for the first time <sup>10)</sup> and found to be very small  $\leq 0.1$  nb.

The measured  $e^+e^- \rightarrow K^+K^-\pi^+\pi^-$  and  $e^+e^- \rightarrow K^+K^-\pi^0\pi^0$  cross sections <sup>11)</sup> are of the order of several nanobarn with an enhancement at 1.7 GeV. In the final state mode  $\phi f_0(980), f_0(980) \rightarrow \pi^+\pi^-, \pi^0\pi^0$  a peak is observed with  $M = 2175 \pm 18$  MeV,  $\Gamma = 58 \pm 2$  MeV and  $\Gamma_{ee} \simeq 2.5$  eV. The new state is named  $Y(2175)$ . It is even more distinctly seen in the final state  $K^+K^-f_0$  (Fig.15). The nature of  $Y(2175)$  is not yet clear. It might be the  $\phi''$  state, a four-quark or molecular ( $ss\bar{s}\bar{s}$ ) state or a light analogue of the known  $Y(4260)$ , because they are both relatively narrow and have close electron widths ( $\Gamma_{ee}(Y(4260)) \simeq 5.5$  eV). If the peak at 2139 MeV in the  $\phi\eta$  channel mentioned above is another decay channel of  $Y(2175)$ , then its electron width should be larger than the quoted 2.5 eV value.

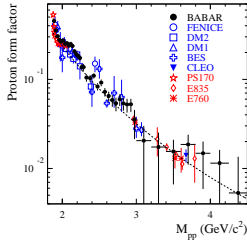


Figure 8: The summary of the proton form factor data and QCD fit.

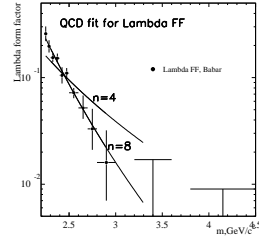


Figure 9: The fitting of  $\Lambda$  form factor data.

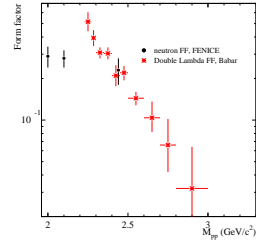


Figure 10: A comparison between doubled  $\Lambda$  and Fenice neutron  $\Lambda$  form factors.

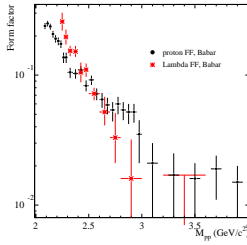


Figure 11: A comparison between proton and  $\Lambda$  form factors.

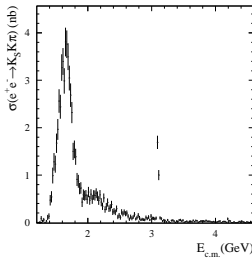


Figure 12: The  $e^+e^- \rightarrow K_S K^\pm \pi^\mp$  cross section.

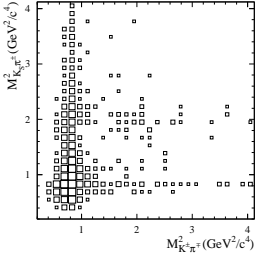


Figure 13: The Dalitz plot for the  $K_S K^\pm \pi^\mp$  state.

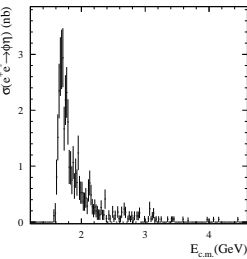


Figure 14: The  $e^+e^- \rightarrow \phi \eta$  cross section.

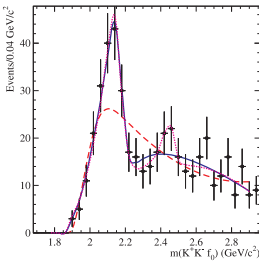


Figure 15: The manifestation of the  $X(2175)$  state.

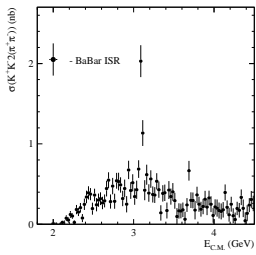


Figure 16: The  $e^+e^- \rightarrow K^+ K^- \pi^+ \pi^- \pi^+ \pi^-$  cross section.

Several new channels with a pair of kaons are studied at Babar [11, 12, 13]:  $e^+e^- \rightarrow K^+K^-K^+K^-$ ,  $K^+K^-\pi^+\pi^-\pi^0$ ,  $K^+K^-\pi^+\pi^-\pi^+\pi^-$ ,  $K^+K^-\pi^+\pi^-\eta$ . In the  $e^+e^- \rightarrow 4K$  process the  $\phi K^+K^-$  intermediate state is dominant. In the  $e^+e^- \rightarrow K^+K^-3\pi$  cross section the  $\omega(783)$  and  $\eta(550)$  are clearly seen in the  $3\pi$  mass spectrum. As an example, the  $e^+e^- \rightarrow K^+K^-4\pi$  cross section is shown in Fig.16. In general, the substructures in all final states with kaons deserve a more careful study.

**Estimation of strangeness contribution to the total hadronic cross section.** The quantity  $R = \sigma(e^+e^- \rightarrow \text{hadrons})/\sigma(e^+e^- \rightarrow \mu^+\mu^-)$ , important in low energy physics, below the charm threshold consists of the contributions of  $u, d, s$  quarks. For the strange quark the relative contribution is 1/6. To calculate  $R$ , the direct cross section measurements are preferable, because the QCD calculations in the non asymptotic region can be not sufficiently precise. Based on the *BABAR* data reported here the total strangeness cross section is summarized at two points 2.5 and 3 GeV and found to be equal to 3.3 and 2.1 nb, respectively. This would be compared with the expected 5 and 3.5 nb of the strangeness cross section and 28 and 19 nb of the total hadronic cross section. So the measured cross sections constitute about 2/3 of the strangeness cross section and 10% of the total hadronic cross section. The rest channels, such as  $K_S K_L \pi$ ,  $K^\pm K_S \pi \pi$ ,  $K_S K_S \pi \pi$  and others can be also measured using the initial state radiation.

**ISR perspectives.** In a few years the total integrated luminosity at B-factories is expected to reach  $\sim 2 \text{ ab}^{-1}$ , that is about 10 times larger than used in the present analysis. This gives hope for more accurate measurements of the reactions considered here and extending the measurements to larger masses.

**Conclusions.** Using the initial state radiation at *BABAR* the cross sections  $e^+e^- \rightarrow p\bar{p}$ ,  $\Lambda\bar{\Lambda}$ ,  $\Sigma^0\bar{\Sigma}^0$ ,  $\Lambda\bar{\Sigma}^0(\Sigma^0\bar{\Lambda})$  are measured. The measured baryon timelike form factors are compared with model predictions. The cross sections with a pair of kaons  $e^+e^- \rightarrow K\bar{K}\pi(\eta)$ ,  $K^+K^-\pi\pi$ ,  $K^+K^-3\pi$ ,  $K^+K^-4\pi$ ,  $K^+K^-K^+K^-$  are also measured. In the  $K^+K^-f_0(980)$  final state, a new state  $Y(2175)$  with  $M = 2175 \pm 18 \text{ MeV}$ ,  $\Gamma = 58 \pm 2 \text{ MeV}$  is observed. The total measured strangeness cross section constitutes about 2/3 of the full strangeness cross section and  $\sim 10\%$  of the total hadronic cross section.

**Acknowledgment.** The author is grateful for fruitful discussions to Vladimir Druzhinin and Victor Chernyak.

## References

1. B.Aubert *et al.* [*BABAR Collaboration*], Nucl. Instr. and Meth. A **479**, 1 (2002)
2. B.Aubert *et al.* [*BABAR Collaboration*], Phys.Rev.D **73**, 012005 (2006), hep-ex/0512023
3. W.F.Wang, Talk given at this Conference
4. D. Bisello *et al.* [*DM2 Collaboration*], Z. Phys. C **48**, 23 (1990)
5. B.Aubert *et al.* [*BABAR Collaboration*], arXiv:0709.1988 v1 [hep-ex]
6. V.L.Chernyak, A.R.Zhitnitsky, JETP Lett. **25**, 510, (1977); G.Lepage, S.Brodsky, Phys. Rev. Lett. **43**, 545 (1977)
7. V.L.Chernyak *et al.* Z. Phys. C - Particles and fields **42**, 569, (1989)
8. A.Antonelli *et al.* Phys. Lett. B **313**, 283 (1993); Nucl. Phys. B **517**, 3, (1998)
9. A.A.Botov *et al.* Nucl. B Phys. (Proc.Suppl.) **162**, 41 (2006)
10. B.Aubert *et al.* [*BABAR Collaboration*], arXiv:0710.4451 [hep-ex]
11. B.Aubert *et al.* [*BABAR Collaboration*], Phys.Rev. D **76**, 012008 (2007), arXiv:0704.0630 [hep-ex]; Phys.Rev. D-RC **74**, 091103 (2006), hep-ex/0610018
12. B.Aubert *et al.* [*BABAR Collaboration*], arXiv:0708.2461 [hep-ex]
13. B.Aubert *et al.* [*BABAR Collaboration*], Phys.Rev. D **73**, 052003 (2006), hep-ex/0602006v1